

- [26] V. A. Daragan, K. H. Mayo, *J. Phys. Chem.* **1996**, *100*, 8378.  
 [27] V. A. Daragan, K. H. Mayo, *J. Phys. Chem. B* **1999**, *103*, 6829.  
 [28] N. Tjandra, S. E. Feller, R. W. Pastor, A. Bax, *J. Am. Chem. Soc.* **1995**, *117*, 12562.  
 [29] B. Brutscher, N. R. Skrynnikov, T. Bremi, R. Brüschweiler, R. R. Ernst, *J. Magn. Reson.* **1998**, *130*, 346.  
 [30] M. W. F. Fischer, L. Zeng, Y. Pang, W. Hu, A. Majumdar, E. R. P. Zuiderweg, *J. Am. Chem. Soc.* **1997**, *119*, 12629.  
 [31] J.-C. Hus, D. Marion, M. Blackledge, *J. Am. Chem. Soc.* **1999**, *121*, 2311.  
 [32] C. Richter, C. Griesinger, I. Felli, P. T. Cole, G. Varani, H. Schwalbe, *J. Biomol. NMR* **1999**, *15*, 241.  
 [33] G. Cornilescu, J. L. Marquardt, M. Ottiger, A. Bax, *J. Am. Chem. Soc.* **1998**, *120*, 6836.  
 [34] J. A. Braatz, M. D. Paulsen, R. L. Ornstein, *J. Biomol. Struct. Dyn.* **1992**, *9*, 935.  
 [35] P. J. Hagerman, B. H. Zimm, *Biopolymers* **1981**, *27*, 1481.  
 [36] S. Vijay-Kumar, C. E. Bugg, W. J. Cook, *J. Mol. Biol.* **1987**, *194*, 531.  
 [37] R. Koradi, M. Billeter, K. Wüthrich, *J. Mol. Graphics* **1996**, *14*, 51.  
 [38] G. Cornilescu, J.-S. Hu, A. Bax, *J. Am. Chem. Soc.* **1999**, *121*, 2949.  
 [39] B. Reif, A. Diener, M. Hennig, M. Maurer, C. Griesinger, *J. Magn. Reson.* **2000**, *143*, 45.  
 [40] R. Sprangers, M. J. Bottomley, J. P. Linge, J. Schultz, M. Nilges, M. Sattler, *J. Biomol. NMR* **2000**, *16*, 47.  
 [41] K. L. Lee, M. Rance, W. J. Chazin, A. G. Palmer, *J. Biomol. NMR* **1997**, *9*, 287.

Received: February 5, 2001 [Z 186]

## Elucidating Changes in Interfacial Water Structure upon Protein Adsorption

Joonyeong Kim and Paul S. Cremer<sup>\*[a]</sup>

### KEYWORDS:

BSA · adsorption · sum-frequency generation · surface chemistry · water chemistry · zeta potential

The adsorption of proteins from solution onto solid surfaces has gained much attention due to its scientific importance<sup>[1–3]</sup> as well as its applications in biofouling,<sup>[4]</sup> food processing,<sup>[5]</sup> biosensor development,<sup>[6]</sup> and the construction of biocompatible materials.<sup>[7]</sup> Previous researchers have used a host of diagnostic methods to study this problem. These include circular dichroism,<sup>[8]</sup> fluorescent microscopy,<sup>[9]</sup> neutron reflectivity,<sup>[10, 11]</sup> surface plasmon resonance spectroscopy,<sup>[12]</sup> attenuated total internal reflection Fourier transform spectroscopy,<sup>[13]</sup> and the quartz

crystal microbalance technique.<sup>[14]</sup> The results have consistently shown that protein adsorption is a complex phenomenon involving a series of dynamic steps from the initial interfacial recruitment to the final structural rearrangements.

Despite these efforts, little is known about the role played by interfacial water in mediating the adsorption process<sup>[15, 16]</sup> because molecular level information from both the substrate surface and protein hydration shells is normally obscured by the contribution of the bulk aqueous solution. This is unfortunate because the role of water is probably crucial. Indeed, protein adsorption at the liquid/solid interface could involve the wholesale realignment of the hydration shells of amino acid residues at the proteins' surface.<sup>[15–17]</sup> Furthermore, substrate-associated water molecules may be heavily disrupted or completely displaced upon the binding of a soluble protein.

Unlike bulk water, interfacial water structure usually exhibits spatial orientation with respect to the underlying surface and thereby lacks inversion symmetry. This fact enables sum-frequency generation (SFG), a surface-specific vibrational spectroscopy, to investigate these buried aqueous interfaces with high selectivity.<sup>[18–20]</sup> Previous nonlinear optical studies of interfacial water structure at the silica/water interface have shown that water ordering is primarily governed by the surface charge density, which is in turn regulated by the bulk pH.<sup>[18, 21]</sup>

In this Communication, we report SFG data on the structure and rearrangement of interfacial water upon bovine serum albumin (BSA) adsorption at the silica/water interface as a function of bulk pH and protein concentration. It is shown that the water structure reorganizes on a timescale that is concomitant with the protein adsorption process and that the molecular ordering of water is highly dependent on the prevailing surface charge density.

The theory and experimental setup of SFG have been described in detail elsewhere.<sup>[22, 23]</sup> We have chosen to study BSA adsorption because both its interfacial behavior<sup>[1, 8, 10, 11, 25]</sup> and structural properties in solution<sup>[24]</sup> have been well characterized.

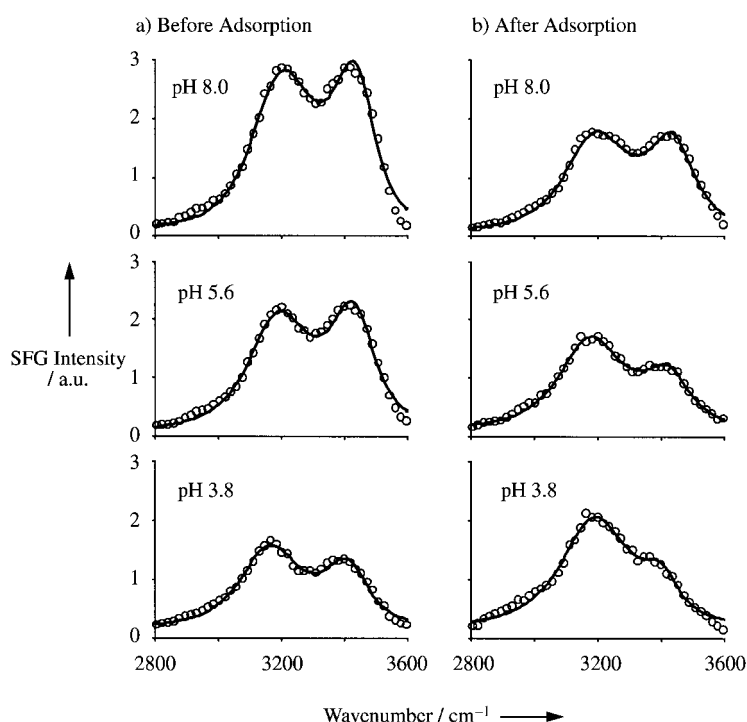
SFG spectra of the silica/water interface in the O–H stretch region before and after BSA adsorption at pH 8.0, 5.6, and 3.8 are shown in Figure 1. The spectra contain two major features. The first peak, located at 3200 cm<sup>−1</sup>, is associated with the OH symmetric stretch of tetrahedrally coordinated water molecules or "ice-like" structure.<sup>[26–28]</sup> The second peak, around 3400 cm<sup>−1</sup>, is from water molecules with less ordered hydrogen bonding or "water-like" structure.<sup>[26, 29]</sup> In Figure 1a, both the ice-like and water-like peak intensities from the bare silica/water interface decreased as the pH was lowered, consistent with previous studies.<sup>[18]</sup>

Figure 1b shows SFG spectra from the silica/water interface after deposition of BSA (1.0 mg mL<sup>−1</sup>) at the corresponding pH values. The effect of adsorption on the intensities of the ice-like and water-like peaks was substantial under all conditions. The fitted data reveal that adsorption of BSA suppressed the oscillator strength of the ice-like and water-like modes at pH 8.0. At pH 5.6, the strength of the ice-like mode was slightly decreased, while the water-like feature showed a substantial reduction in intensity. By lowering the pH to 3.8, the intensity of

[a] Prof. P. S. Cremer, J. Kim  
 Department of Chemistry  
 Texas A&M University  
 P.O. Box 30012, College Station, TX 77842-3012 (USA)  
 Fax: (+1) 979-845-7561  
 E-mail: cremer@mail.chem.tamu.edu



Supporting information for this article is available on the WWW under <http://www.chemphyschem.com> or from the author.



**Figure 1.** SFG spectra in the O–H stretch region at the silica/water interface a) before and b) after adsorption of BSA from a  $1.0 \text{ mg mL}^{-1}$  solution at various pH values. Circles denote collected data while the solid lines represent fitted data using a Voigt profile.

the ice-like mode increased while that of the water-like mode decreased.

Significantly, the changes in intensities of the ice-like peak in the presence of the BSA layer follow the trend of changes in the surface charge density. Previous studies have shown that the surface  $\xi$ -potential is significantly altered by BSA adsorption.<sup>[30]</sup> In particular, adsorption at pH 8.0 leads to a small reduction in surface  $\xi$ -potential. A much larger reduction is expected as the isoelectric point (IEP of BSA is at pH 4.7)<sup>[24]</sup> is approached because most of the electrostatic repulsion between the proteins have been eliminated leading to increased surface coverage. Finally, below its isoelectric point, BSA bears a net positive charge that can overcompensate for the original surface charge. This is the case at pH 3.8, where the absolute value of the  $\xi$ -potential is substantially increased by BSA adsorption, but has the opposite sign from the bare surface.<sup>[30, 31]</sup> The low-pH situation is analogous to changes in surface potential during layer-by-layer polyelectrolyte film growth on an oppositely charged substrate.<sup>[32]</sup>

By contrast with the ice-like feature, the intensities of the water-like peaks were reduced upon BSA adsorption over the entire pH range investigated. One possible explanation is that adsorbed protein mainly disrupts and displaces the outermost water layers that are primarily responsible for the water-like peak. Indeed, this notion is consistent with the proposal that a solute depletion layer exists between adsorbed protein and a hydrophilic silica surface.<sup>[15]</sup>

To investigate concentration effects, the amount of BSA in the bulk solution was varied from  $0.04$  to  $1.0 \text{ mg mL}^{-1}$ . SFG signal intensity was monitored at  $3200 \text{ cm}^{-1}$  (ice-like peak) as a

function of time while flowing each protein solution through the flow cell. The results are shown in Figure 2. At pH 8.0, the SFG intensity attenuated over a period of  $2000$ – $3000 \text{ s}$  before reaching a new steady-state value. This timescale is in good agreement with previous results measuring the kinetics of protein deposition.<sup>[33]</sup> The final SFG intensity depended on the bulk BSA concentration with greater and faster signal reduction observed at the highest protein concentration. By lowering the pH to 5.6, signal reduction became faster ( $300$ – $1000 \text{ s}$ ). The rate of change was only slightly dependent on the BSA concentration and the final SFG intensities appeared to be almost completely concentration independent. At pH 3.8, the SFG signal increased within  $100 \text{ s}$ . Both its rate of increase and

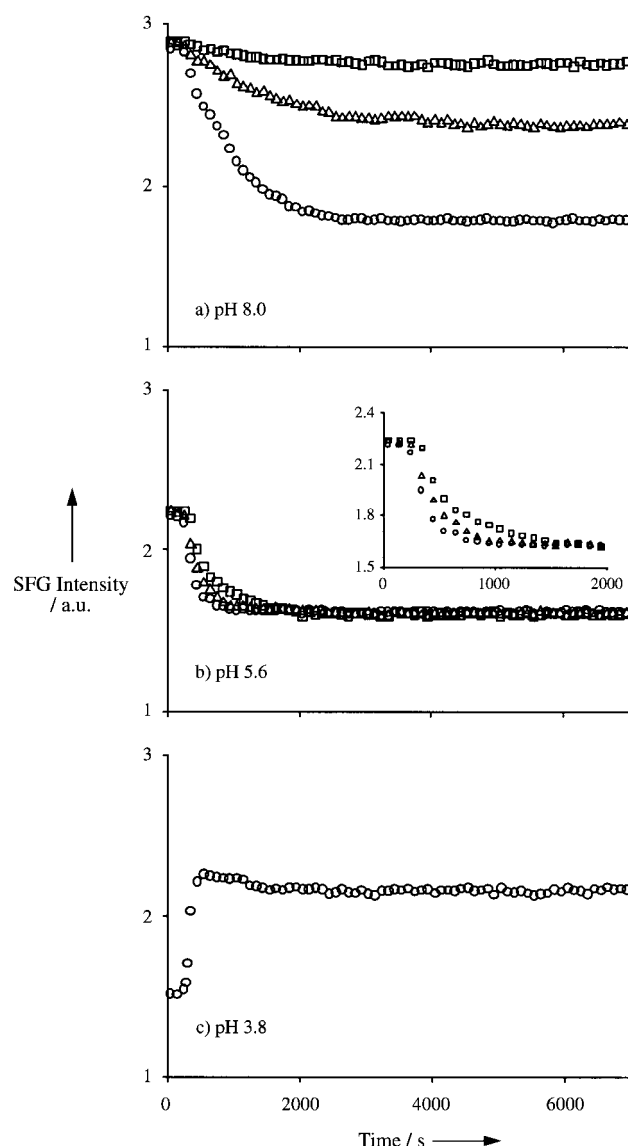


**Figure 2.** SFG intensity at  $3200 \text{ cm}^{-1}$  was monitored during the adsorption of BSA at pH values of a) 8.0, b) 5.6, and c) 3.8. The BSA was introduced at  $t = 100 \text{ s}$  and flowed for  $100 \text{ s}$ . The protein solution was kept in contact with the interface for  $1 \text{ h}$  and then removed by washing. The concentrations of the BSA solutions are  $1.0$  ( $\circ$ ),  $0.2$  ( $\triangle$ ), and  $0.04 \text{ mg mL}^{-1}$  ( $\square$ ). Lower concentrations exactly overlapped the data at  $1.0 \text{ mg mL}^{-1}$  in (c) and are not shown due to excessive crowding. The inset in (b) focuses on the  $t < 2000 \text{ s}$ .

final value were the same regardless of the BSA concentration employed over the range investigated.

The entire vibrational spectrum in the O–H stretch range was taken at each concentration at the end of the adsorption process and the spectra at pH 8.0 are shown in Figure 3. As can be clearly seen, both the ice-like and water-like modes were attenuated as the concentration of BSA was increased.

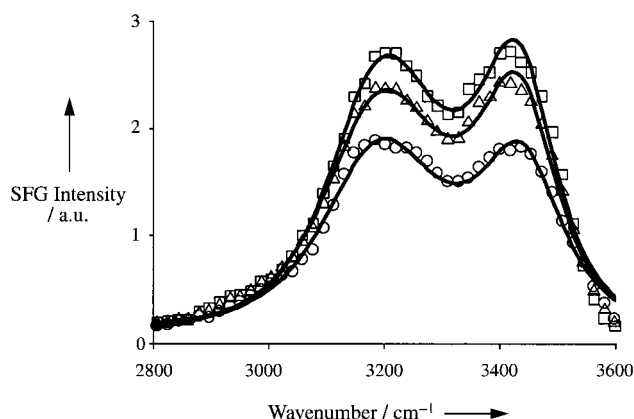


**Figure 3.** SFG spectra in the O–H stretch region at the silica/water interface after adsorption of BSA from 1.0 (○), 0.2 (△), and 0.04 mg mL<sup>−1</sup> (□) solutions at pH 8.0. Solid lines are fitted data.

Several factors are known to influence the rate of protein deposition. These include the charge on the substrate and protein as well as the protein's concentration and conformation. At pH 8.0, both the BSA and substrate are negatively charged and the adsorption process is slow. Therefore, at low bulk concentration the first BSA molecules to become adsorbed have ample opportunity to spread out over the surface without interference from neighboring proteins. As the concentration is increased, spreading becomes limited by competition from adjacent species.<sup>[9, 34]</sup> This limits the total footprint for each molecule, but increases the absolute amount of protein that can be adsorbed. The  $\xi$ -potential decreases as the coverage rises.<sup>[33]</sup> This is consistent with our data, which show greatest attenuation of the SFG signal at the highest protein concentration (Figure 3).

At pH 5.6, the BSA and silica both bear less negative charges and the rate of protein adsorption is enhanced with respect to pH 8.0, thus greatly reducing the time required to achieve full surface coverage (Figure 2b). There are still some small differences in adsorption rates as the protein concentration is changed as supported by the differences in the time-dependent SFG data. The spreading process, however, is sufficiently slow that the ultimate amount of protein adsorbed is relatively unaffected. Below the isoelectric point, adsorption is rapid due to the electrostatic attraction with the surface, which is quickly saturated with protein at all concentrations investigated (Figure 2c).

Another factor that affects the adsorption rate is the conformation of BSA. Previous studies have shown that BSA molecules with less  $\alpha$ -helical content can adsorb faster than native BSA.<sup>[1, 8, 25]</sup> Generally, BSA becomes less compact and has less  $\alpha$ -helical content as the pH is lowered.<sup>[24]</sup> One might,

therefore, expect that adsorption would be more facile at lower pH even without electrostatic considerations.

In a final set of experiments, we checked for the presence of an O–H stretch peak near 3670 cm<sup>−1</sup>, which typically appears at a hydrophobic/aqueous interface.<sup>[35]</sup> No significant intensity was observed in this region upon protein adsorption (data not shown). This result is consistent with the idea that structural rearrangements of adsorbed BSA take place in a manner that avoids exposure of the hydrophobic core of the macromolecule to the aqueous phase.

In summary, interfacial water structure was investigated upon the deposition of BSA at the silica/water interface by employing SFG vibrational spectroscopy. Changes in interfacial water structure appeared to correlate with variations in the surface  $\xi$ -potential and provided evidence for a solute depletion layer. Furthermore, changes in interfacial water structure took place over a timescale that corresponded to the protein adsorption process.

## Experimental Section

SFG spectra were obtained with a passive–active mode-locked Nd:YAG laser (PY61c, Continuum) equipped with a negative feedback loop in the oscillator cavity to provide enhanced shot-to-shot stability. The SFG signal generated from the sample was collected by a photomultiplier tube, sent to a gated integrator, and stored digitally. All spectra presented in this paper were collected with the  $S_{\text{SFG}}$ ,  $S_{\text{vis}}$ , and  $P_{\text{IR}}$  polarization combination. For each scan, data were collected in 6 cm<sup>−1</sup> increments in the 2800–3600 cm<sup>−1</sup> range.

Ultrapure water (minimum resistivity 18 m $\Omega$  cm, NANOpure, Barnstead) was used in the preparation of phosphate buffer solutions and in cleaning the apparatus. BSA (99%, Sigma) was purified by gel chromatography (Sephadex G-100, Sigma) before use. BSA solutions at 1.0, 0.2, and 0.04 mg mL<sup>−1</sup> were prepared and adjusted with sodium phosphate to pH 3.8, 5.6, and 8.0. The concentration of BSA was confirmed by UV absorption at 280 nm using the extinction coefficient 0.667 g L<sup>−1</sup>.<sup>[24]</sup> Appropriate amounts of AR grade NaCl were subsequently added to raise the total ionic strength to 32 mM; BSA contributed less than 1.0 mM to this value.

IR-grade fused silica windows (diameter 25 mm, thickness 1.6 mm) were purchased from Quartz Plus Inc., cleaned in hot chromic acid solution for several hours, rinsed with copious quantities of purified water, and baked in a kiln at 400 °C overnight before use.

SFG measurements were carried out using a homemade flow-cell (volume  $\approx$  2.0 mL), that consisted of a machined Teflon body fitted with a fused silica plate. BSA adsorption was carried out by flowing 20 mL of the appropriate BSA solution (circa 100 s), stopping the flow for 3600 s, followed by rinsing with an excess amount of BSA-free solution at the same pH and ionic strength. The volume of the flow cell employed in these experiments was large enough that no significant depletion of the bulk protein concentration occurred even for the 0.04 mg mL<sup>−1</sup> BSA solution.

*This work was generously supported by the Petroleum Research Fund through Grant 34149-G5, a Research Innovation Award from the Research Corporation of America through Grant RI0437, the Robert A. Welch Foundation through Grant A-1421, and startup funds from Texas A&M University.*

- [1] W. Norde, *Cell Mater.* **1995**, 5, 97.
- [2] "Proteins at Interfaces: Physicochemical and Biochemical Studies": T. A. Horbett, J. L. Brash, *ACS Symp. Ser.* **1995**, 602, 1.
- [3] "Protein Adsorption": J. D. Brash, *Surface and Interfacial Aspects of Biomedical Polymers, Vol. 2*, Plenum, New York, NY, **1985**.
- [4] C. Sandu, R. K. Singh, *Food Technol.* **1991**, 45, 84.
- [5] J. McGuire, V. Krisdhasima, *Food Technol.* **1991**, 45, 92.
- [6] G. A. Rechnitz, *Chem. Eng. News* **1988**, 66(36), 24.
- [7] J. A. Hubbell, *Bio-Technol.* **1995**, 13, 565.
- [8] W. Norde, C. E. Giacomelli, *Macromol. Symp.* **1999**, 145, 125.
- [9] C. F. Wertz, M. M. Santore, *Langmuir* **1999**, 15, 8884.
- [10] T. J. Su, J. R. Lu, R. K. Thomas, Z. F. Cui, J. Penfold, *J. Phys. Chem. B* **1998**, 102, 8100.
- [11] T. J. Su, J. R. Lu, R. K. Thomas, Z. F. Cui, *J. Phys. Chem. B* **1999**, 103, 3727.
- [12] G. B. Sigal, M. Mrksich, G. M. Whitesides, *J. Am. Chem. Soc.* **1998**, 120, 3464.
- [13] S. Servagent-Noirville, M. Revault, H. Quiquampoix, M. H. Baron, *J. Colloid Interface Sci.* **2000**, 221, 273.
- [14] B. S. Murray, C. Deshaies, *J. Colloid Interface Sci.* **2000**, 227, 32.
- [15] a) E. A. Vogler, *Adv. Colloid Interface Sci.* **1998**, 74, 69; b) E. A. Vogler, *J. Biomater. Sci. Polym. Ed.* **1999**, 10, 1015.
- [16] J. Israelachvili, H. Wennerström, *Nature* **1996**, 379, 219.
- [17] N. Nandi, K. Bhattacharyya, B. Bagchi, *Chem. Rev.* **2000**, 100, 2013.
- [18] Q. Du, E. Freysz, Y. R. Shen, *Phys. Rev. Lett.* **1994**, 72, 238.
- [19] D. E. Gragson, G. L. Richmond, *J. Am. Chem. Soc.* **1998**, 120, 366.
- [20] S. Baldelli, C. Schnizer, D. J. Campbell, M. J. Shultz, *J. Phys. Chem. B* **1999**, 103, 2789.
- [21] S. Ong, X. Zhao, K. B. Eisenthal, *Chem. Phys. Lett.* **1992**, 191, 327.
- [22] Y. R. Shen, *Nature* **1989**, 337, 519.
- [23] Y. R. Shen, *Surf. Sci.* **1994**, 299/300, 551.
- [24] T. J. Peters, *All About Albumin Biochemistry, Genetics, and Medical Applications*, Academic Press, San Diego, CA, **1996**.
- [25] W. Norde, J. P. Favier, *Colloids Surf.* **1992**, 64, 87.
- [26] D. Eisenberg, W. Kauzmann, *The Structure and Properties of Water*, Oxford University Press, New York, NY, **1969**.
- [27] G. E. Walrafen in *Water—A Comprehensive Treatise, Vol. 1* (Ed.: F. Franks), Plenum, New York, NY, **1972**, p. 151.
- [28] M. R. Yalamanchili, A. A. Atia, J. D. Miller, *Langmuir* **1996**, 12, 4176.
- [29] P. A. Giguere, *J. Raman Spectrosc.* **1984**, 15, 354.
- [30] A. V. Elgersma, R. L. J. Zsom, W. Norde, J. Lyklema, *J. Colloid Interface Sci.* **1990**, 138, 145.
- [31] W. Norde, J. Lyklema, *J. Colloid Interface Sci.* **1978**, 66, 277.
- [32] G. Ladam, P. Schaaf, J. C. Voegel, P. Schaaf, G. Decher, F. Cuisinier, *Langmuir* **2000**, 16, 1249.
- [33] P. V. Dulm, W. Norde, *J. Colloid Interface Sci.* **1983**, 91, 248.
- [34] R. R. Seigel, P. Harder, R. Dahint, M. Grunze, F. Josse, M. Mrksich, G. M. Whitesides, *Anal. Chem.* **1997**, 69, 3321.
- [35] Q. Du, E. Freysz, Y. R. Shen, *Science* **1994**, 264, 826.

Received: January 26, 2001 [Z181]

## The Diode Behavior of Asymmetrically Ordered Au<sub>55</sub> Clusters

Viktoria Torma,<sup>[a]</sup> Torsten Reuter,<sup>[a]</sup>  
Olivia Vidoni,<sup>[a]</sup> Matthias Schumann,<sup>[b]</sup>  
Christian Radehaus,<sup>[b]</sup> and Günter Schmid<sup>\*,[a]</sup>

### KEYWORDS:

cluster compounds • diodes • monolayers • thin films

Nanoclusters, organized in two-dimensional lattices, provide excellent model systems for nanoelectronic devices.<sup>[1–3]</sup> Ligand-stabilized Au<sub>55</sub> clusters, 1.4 nm in diameter, have frequently turned out to act as single-electron transistors, even at room temperature.<sup>[4, 5]</sup> Since we recently succeeded in generating perfectly ordered monolayers of [Au<sub>55</sub>(PPh<sub>3</sub>)<sub>12</sub>Cl<sub>6</sub>] clusters,<sup>[6, 7]</sup> the electronic properties of such two-dimensional lattices can be studied systematically.<sup>[8]</sup> Herein we report the first electrical measurements on two-dimensional cluster networks which should be of decisive significance for future nanoelectronic applications.

In our very first attempt to receive information on the conductivity behavior of Au<sub>55</sub> monolayers, we placed cluster monolayers on two tungsten electrodes, 50–150 nm apart and 25 nm in height, which sat on a silica platelet. These electrodes have been fabricated by electron-beam lithography.<sup>[9]</sup> The monolayers were prepared as described by us in the literature.<sup>[7]</sup> To generate them between the electrodes, the SiO<sub>2</sub> platelet equipped with the electrodes was dipped into a very dilute aqueous solution of polyvinylpyrrolidone (PVP), followed by addition of a thin film of a dichloromethane solution of the clusters on top of the water surface. The platelet was then carefully pulled out at an angle of approximately 20° and dried in air. In most cases the electrodes were linked by a closed cluster monolayer. To check whether the electrode monolayer system was perfect we used scanning electron microscopy (SEM). Because of charging effects in the PVP layer, SEM does not allow the resolution of individual clusters, however, it is sufficiently suited to detect closed areas of clusters between the electrodes. Figure 1 shows the SEM image of the tungsten electrodes on the SiO<sub>2</sub> surface. Islands of cluster monolayers can easily be detected as light gray areas. From separate investigations,<sup>[7]</sup> we know that in case of monolayer formation the clusters

[a] Prof. Dr. G. Schmid, Dipl.-Chem. V. Torma, Dipl.-Chem. T. Reuter, Dr. O. Vidoni  
Institut für Anorganische Chemie  
Universität Essen  
Universitätsstrasse 5–7, 45117 Essen (Germany)  
Fax: (+49) 201-183-4195  
E-mail: guenter.schmid@uni-essen.de

[b] Dr. M. Schumann, Prof. Dr. C. Radehaus  
Technische Universität Chemnitz  
Fakultät für Elektrotechnik und Informationstechnik  
09107 Chemnitz (Germany)